A three-step kinetic mechanism for selective inhibition of cyclo-oxygenase-2 by diarylheterocyclic inhibitors

Mark C. WALKER[1], Ravi G. KURUMBAIL, James R. KIEFER, Kirby T. MORELAND, Carol M. KOBOLDT, Peter C. ISAKSON, Karen SEIBERT and James K. GIERSE

Searle Discovery Research, Pharmacia Corp., 700 Chesterfield Parkway N., St Louis, MO 63198, U.S.A.

Cyclo-oxygenase (COX) enzymes are the targets for non-steroidal anti-inflammatory drugs (NSAIDs). These drugs demonstrate a variety of inhibitory mechanisms, which include simple competitive, as well as slow binding and irreversible inhibition. In general, most NSAIDs inhibit COX-1 and -2 by similar mechanisms. A unique class of diarylheterocyclic inhibitors has been developed that is highly selective for COX-2 by virtue of distinct inhibitory mechanisms for each isoenzyme. Several of these inhibitors, with varying selectivity, have been utilized to probe the mechanisms of COX inhibition. Results from analysis of both steady-state and time-dependent inhibition were compared. A generalized mechanism for inhibition, consisting of three sequential reversible steps, can account for the various types of kinetic behaviour observed with these inhibitors.

Key words: celecoxib, meloxicam, PGH_2 synthase, prostaglandin, valdecoxib.

INTRODUCTION

Cyclo-oxygenase (COX) enzymes catalyse the first committed step in the biosynthesis of prostaglandins (PGs) and thromboxanes, and are the pharmacological targets of non-steroidal anti-inflammatory drugs (NSAIDs) (for reviews see [1–5]). Two isoforms of COX have been identified that share approximately 60 % sequence identity and whose expression is subject to distinct transcriptional regulation. One isoform, designated COX-1, is expressed in nearly all tissues and is thought to be responsible for the production of prostanoids at basal levels for the maintenance of physiological homoeostasis [6]. Another isoform, designated COX-2, is expressed in response to inflammatory stimuli and is primarily responsible for the dramatic increase in PG production observed at sites of inflammation. The inhibition of COX-2-derived PG production is thought to be responsible for the antipyretic, anti-inflammatory and analgesic properties of NSAIDs [7,8]. However, most NSAIDs are relatively non-selective, inhibiting COX-1, as well as COX-2 [9,10]. Adverse side effects, such as increased incidence of gastric ulceration and renal complications, associated with the chronic administration of NSAIDs, are thought to arise as a consequence of the inhibition of COX-1 [11]. The discovery of distinct COX isoforms and the subsequent cloning and expression of these isoforms has permitted the development of a novel class of diarylheterocyclic COX inhibitors that are selective for COX-2 [12–16]. These new inhibitors provide the therapeutic benefit of traditional NSAIDs without the adverse side effects normally associated with chronic NSAID use.

The inhibition of COX isoenzymes by NSAIDs generally conforms to one of three inhibitory mechanisms: simple reversible inhibition, as demonstrated by ibuprofen [17]; time-dependent reversible inhibition, which includes both weaker binding inhibitors, such as naproxen [18], and tight binding inhibitors, such as indomethacin and meclofenamic acid [17]; and irreversible covalent inhibition, as demonstrated by aspirin [19] and *o*-(acetoxy-phenyl)hept-2-ynyl sulphide ('APHS') [20]. Most of the traditional NSAIDs display similar inhibitory mechanisms against both COX-1 and COX-2 [5,18,21,22], and are relatively non-selective. However, COX-2-selective diarylheterocyclic inhibitors demonstrate distinct inhibitory mechanisms for the two isoforms [15,18,23,24]. For example, celecoxib (Figure 1) has been reported to be a reversible competitive inhibitor of COX-1 while demonstrating time-dependent irreversible inhibition of COX-2. The contribution of a slow irreversible process to the inhibition of COX-2, but not COX-1, accounts for the potency and selectivity demonstrated by members of this structural class.

In a previous communication [18], the kinetics for steady-state and time-dependent inhibition of COX isoforms by one of these selective inhibitors, celecoxib, were reported and compared with those obtained with other NSAIDs. The data obtained with celecoxib suggested that the mechanism of inhibition by this class of compounds is more complex than was previously recognized. Fluorescence quenching results obtained following the rapid mixing of a fluorescent diarylheterocycle, SC-66299, with COX-2 have suggested a three-step kinetic process for the association of inhibitor with COX-2 [25]. In contrast, the binding of this inhibitor to COX-1 appeared to be comprised of two distinct steps, despite previous reports that COX-1 inhibition by this class of inhibitor is strictly competitive.

In the present study, several representative diarylheterocycles have been utilized to probe the mechanism of COX inhibition by NSAIDs. Both COX-1- and COX-2-selective inhibitors have been evaluated to examine the basis for potency and selectivity against COX isoforms. The results suggest a minimal mechanism that includes three steps. Reversible association of these inhibitors with COX is comprised of two steps that may or may not appear kinetically distinct, depending on the relative magnitudes of the respective rate constants. Selectivity for COX-2 is derived from the contribution of a third irreversible step that is exploited most effectively by those diarylheterocyclic inhibitors containing a phenylsulphonamide or a phenylsulphone moiety. A COX-1-selective diarylheterocycle, SC-560, lacks the chemical moiety common to COX-2-selective inhibitors and demonstrated kinetic behaviour consistent with a model in which an irreversible step

Abbreviations used: COX, cyclo-oxygenase; NSAIDs, non-steroidal anti-inflammatory drugs; PGs, prostaglandins.

[1] To whom correspondence should be addressed (e-mail mark.c.walker@pharmacia.com).

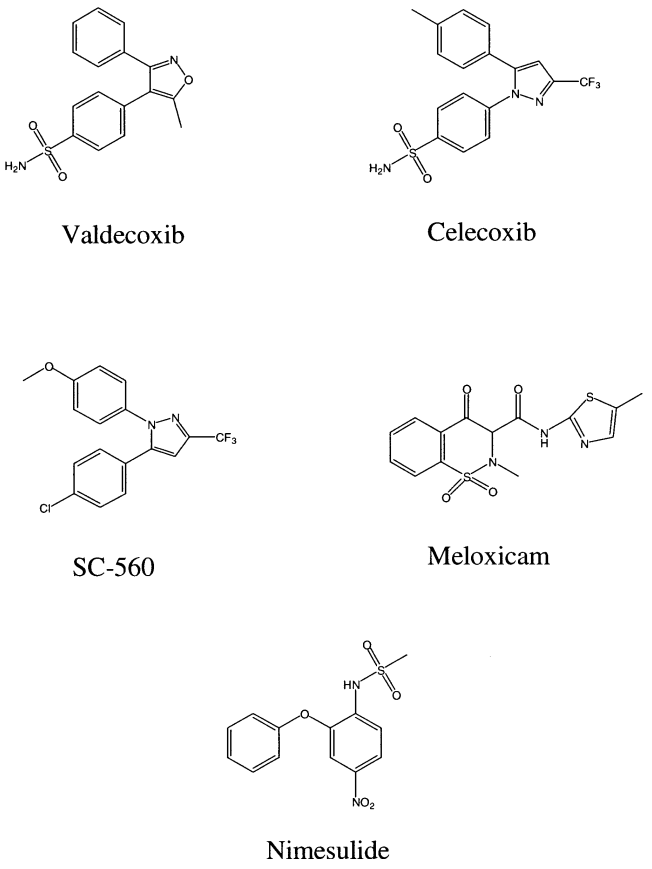

Figure 1 Structures of COX inhibitors utilized in the present study

does not contribute to the inhibition of COX-1. This compound derives potency and selectivity for COX-1 by taking advantage of the second reversible step differentially for the two isoenzymes. This three-step mechanism is interpreted in the light of structural information derived from X-ray crystallography and provides a basis for the proposal of a working model for COX inhibition.

MATERIALS AND METHODS

Materials

Phenol, haematin, Tween 20, diethyldithiocarbamate and all standard buffer reagents were obtained from Sigma (St Louis, MO, U.S.A.). Arachidonic acid was obtained as the sodium salt from Nu-Chek Prep (Elysian, MN, U.S.A.). Nimesulide was obtained from Sigma. Meloxicam and all other inhibitors were prepared and supplied by the Medicinal Chemistry Department (Searle Discovery Research). Valdecoxib was prepared as described by Talley [26]. Other diarylheterocyclic inhibitors were prepared as described by Penning et al. [14]. Inhibitor stocks were prepared in DMSO. COX-1 from sheep seminal vesicles and recombinant murine COX-2 were purified as previously described [18]. Water was Milli-Q purified (Millipore, Bedford, MA, U.S.A.).

Enzyme assays

Enzymic activity was monitored continuously, following the consumption of molecular O_2 using a Clark-style polarographic electrode in a 600 μl reaction vessel (Model 203B; Instech Labs, Plymouth Meeting, PA, U.S.A.). Data were collected using a PC

$$E + I \underset{k_{-1}}{\overset{k_1}{\rightleftharpoons}} [EI] \xrightarrow{k_{inact}} EI^*$$

Scheme 1 Two-step irreversible mechanism

equipped with a Keithley DAS-8 data acquisition board (Kiethley Instruments, Taunton, MA, U.S.A.). The total μmol of O_2 and the rate of change in O_2 concentration, expressed as μmol of O_2 consumed/min, were obtained from the first derivative of $[O_2]$ versus time using vendor supplied software (INTAKE.EXE; Instech Labs). Maximal rates were typically achieved within 3–4 s after initiating the enzymic reaction.

The assay buffer consisted of 100 mM Tris/HCl (pH 8.1) containing 1 μM haem, 0.5 μM phenol and air saturated O_2 concentrations (approx. 200 μM) pre-equilibrated at 37 °C. Enzyme stock solutions were pre-equilibrated with a slight molar excess of haemin in order to insure reconstitution to the holoform and were stored on ice. Arachidonate and inhibitor were introduced as 6 μl aliquots of a 100-fold concentrated stock solution into the reaction vessel containing assay buffer [1 % (v/v) DMSO, final concn]. Assay mixtures were allowed to equilibrate in the reaction vessel at 37 °C for several minutes in order to permit the electrode response to stabilize. During the analysis of steady-state inhibition, the reaction was initiated by the addition of 10–15 μl of enzyme stock (10–40 μg/ml, final concn).

Statistical calculations

For the analysis of steady-state inhibition, the enzymic reaction was initiated by the addition of 10–15 μl of enzyme stock (10–40 μg/ml, final concn) to a pre-equilibrated reaction mixture containing substrate and inhibitor. Maximal rates of O_2 consumption obtained in the absence of a preincubation with inhibitor were utilized for non-linear least-squares fitting to mathematical models for competitive, non-competitive or mixed inhibition using the program GraFit v 4.0.1 [27]. The reported apparent K_i values were obtained under conditions of air saturated aqueous O_2 concentrations at 37 °C.

For the analysis of time-dependent inhibition, enzyme and inhibitor were preincubated at 37 °C for 2 s to 3 min before initiating the enzymic reaction by the addition of 6 μl of 10 mM arachidonate (100 μM, final concn). Maximal rates of O_2 consumption were referenced to that of control assays performed in the absence of inhibitor and are expressed as the percentage of activity remaining. Irreversible time-dependent inhibition was evaluated based upon a two-step model of a reversible second-order reaction followed by an irreversible first-order reaction [17,23,28,29], as illustrated by Scheme 1. The time-dependent loss of enzymic activity is described by:

$$A_t = A_0 \times e^{-(k_{obs} \times t)} \quad (1)$$

which represents a monoexponential decay, where A_t equals the enzymic activity remaining following preincubation time (t) and the observed rate of decay is represented by k_{obs}. The dependence of the observed rate on inhibitor concentration is defined as:

$$k_{obs} = \frac{k_{inact} \times I}{(K_I + I)} \quad (2)$$

where k_{inact} corresponds to the limiting rate for irreversible inhibition and K_I corresponds to the concentration of inhibitor that results in a rate equal to half of the limiting rate [28].

$$E + I \underset{k_{-1}}{\overset{k_1}{\rightleftharpoons}} [EI] \underset{k_{-2}}{\overset{k_2}{\rightleftharpoons}} [EI^*]$$

Scheme 2 Two-step reversible mechanism

Reversible time-dependent inhibition was evaluated based upon a two-step model of a reversible second-order reaction followed by a reversible first-order reaction, as illustrated by Scheme 2. The time-dependent loss of enzymic activity is described by:

$$A_t = (A_0 - B) \times e^{-(k_{obs} \times t)} + B \quad (3)$$

which represents a monoexponential decay that approaches a non-zero asymptote.

The value B in eqn (3) reflects the final equilibrium established following prolonged preincubation of enzyme with inhibitor ($t = \infty$) and is represented by [30]:

$$B = (A_0 \times k_{-2})/k_{obs} \quad (4)$$

Estimates for k_2 and k_{-2} were obtained from global fitting of data obtained at various preincubation times and at various inhibitor concentrations to the following equation:

$$A_t = A_0 \times [(1 - k_{-2}/k_{obs}) \times e^{-(k_{obs} \times t)} + k_{-2}/k_{obs}] \quad (5)$$

where k_{obs} is equal to the sum of the forward and reverse rates, i.e.:

$$k_{obs} = \frac{k_3 \times I}{(K_i + I)} + k_{-2} \quad (6)$$

The constant A_0 is defined as:

$$A_0 = \frac{(K_m + S)}{[K_m \times (1 + I/K_i) + S]} \quad (7)$$

in order to approximate the extent of inhibition observed at zero time, based upon a model for competitive inhibition. Values for K_m and K_i obtained from steady-state kinetic measurements were provided as constants. The Michaelis constants for arachidonate used during global fitting were 35 μM for COX-1 and 20 μM for COX-2.

RESULTS

Valdecoxib is an example of a COX-2-selective diarylheterocycle containing a central isoxazole ring (Figure 1). In Figure 2 direct plots of maximal rate versus substrate concentration obtained from an examination of the steady-state inhibition of COX-1 and COX-2 by valdecoxib are presented. These data were fitted to a kinetic model for competitive inhibition, providing K_i values of 24 and 20 μM for COX-1 and COX-2 respectively. A kinetic model for competitive inhibition is consistent with results from X-ray crystallography, demonstrating the association of valdecoxib within the active site of murine COX-2 (R. G. Kurumbail, J. R. Kiefer, J. L. Pawlitz, A. M. Stevens, R. A. Stegeman, W. C. Stallings and J. K. Gierse, unpublished work). The comparable K_i values obtained with COX-1 and COX-2 suggest that the initial binding interactions that occur during steady-state experiments are similar for both isoforms.

In the case of COX-1, a systematic deviation between observed and fitted values was apparent at higher substrate concentrations (Figure 2a). This deviation demonstrated an inhibitory effect on V_{max}, which could not be adequately accounted for using a model for competitive inhibition. It was found that the observed data

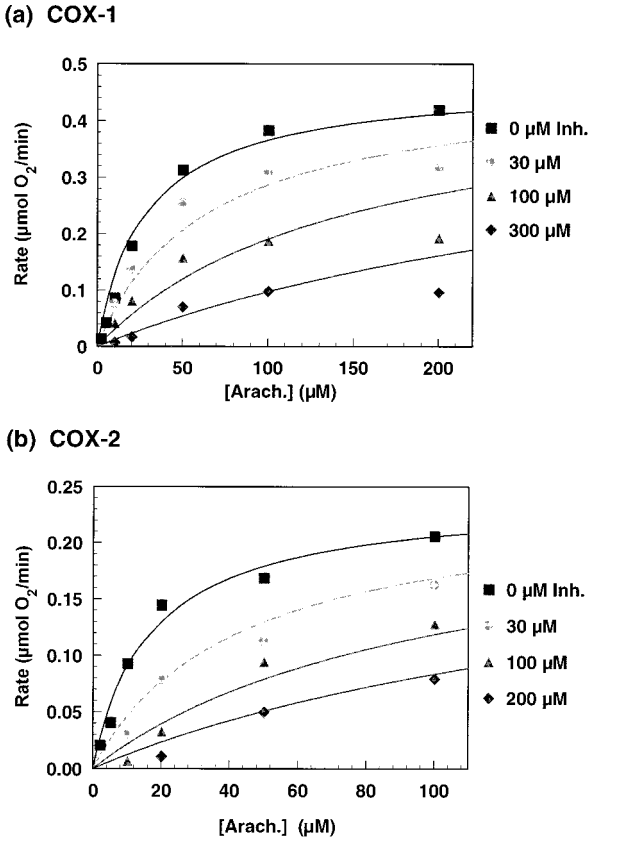

Figure 2 Direct plots of the maximal rate of O_2 consumption/min as a function of substrate concentration obtained at various concentrations of valdecoxib with either (a) COX-1 or (b) COX-2

Reactions were initiated by the addition of enzyme to reaction mixtures containing substrate and inhibitor pre-equilibrated at 37 °C. Maximal rates were generally achieved within 3 s following the addition of enzyme. The curves drawn represent the fit of the data to a model for competitive inhibition. Deviations between observed and fitted results are discussed in the text. Arach., arachidonate; Inh., inhibitor.

were better fitted to a model for non-competitive inhibition ($P = 0.023$). Non-competitive inhibition would imply that the inhibitor binds at a site independent of the substrate binding site. However, there is no supporting evidence for the presence of an alternative binding site for valdecoxib. It should be noted that slow reversible binding interactions can also give rise to kinetic behaviour, which could be misinterpreted as non-competitive inhibition [31]. This point will be addressed further in the Discussion section.

The time-dependent inhibition of COX-1 and COX-2 by valdecoxib was also examined (Figure 3). Preincubation of inhibitor with enzyme appeared to have no effect on the inhibitory potency of valdecoxib towards COX-1 (Figure 3a). However, valdecoxib demonstrated a slow progressive increase in potency against COX-2 as a function of preincubation time (Figure 3b). This difference in time-dependent inhibition of COX-1 and COX-2 by diarylheterocycles has been observed previously [15,18,23,29], and serves as the basis for their selectivity for COX-2 *in vitro* and *in vivo*. The time-dependent behaviour observed with valdecoxib is described as a monoexponential decay of COX-2 activity as a function of preincubation time that extrapolates to complete loss of activity. This behaviour is consistent with an irreversible process, as illustrated by Scheme 1. The observed rate constant for this decay process was

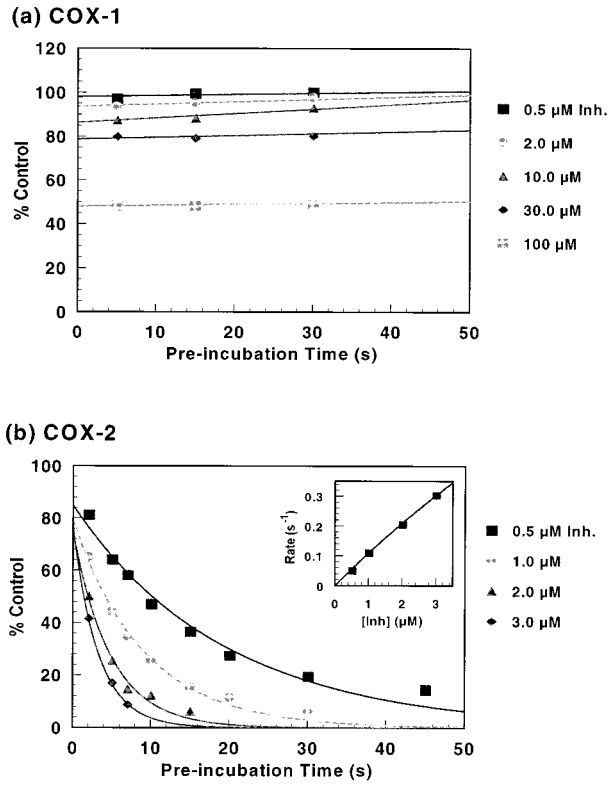

Figure 3 Time-dependent inhibition of (a) COX-1 and (b) COX-2 by valdecoxib

Enzyme and inhibitor (Inh.) were preincubated at 37 °C for the indicated times and the reaction was initiated by the addition of 100 μM arachidonate (final concn). The activity remaining is expressed relative to controls obtained in the absence of inhibitor. The curves drawn in (**b**) represent fits to a monoexponential decay to the baseline, as defined by eqn (1). The inset in (**b**) describes the relationship between k_{obs} obtained from fitting and the corresponding inhibitor concentration. The line drawn represents the fit of the data to eqn (2).

Table 1 Comparison of kinetic constants for competitive and time-dependent inhibition by diarylheterocycles and selected NSAIDs

Abbreviation: n.d., not determined.

Inhibitor	COX-1	COX-2
Valdecoxib		
Steady-state K_i (μM)	24.0 ± 5.5	20.0 ± 3.1
Time-dependent K_i (μM)	–	35.0 ± 6.1
k_{inact} (s^{-1})	–	3.80 ± 0.63
Celecoxib		
Steady-state K_i (μM)	4.20 ± 0.66	14.0 ± 0.5
Time-dependent K_i (μM)	–	3.0 ± 0.6
k_{inact} (s^{-1})	–	0.39 ± 0.05
SC-560		
Steady-state K_i (μM)	0.10 ± 0.01	1.80 ± 0.26
k_2 (s^{-1})	n.d.	n.d.
k_{-2} (s^{-1})	n.d.	n.d.
Meloxicam		
Steady-state K_i (μM)	430 ± 82	1150 ± 360
k_2 (s^{-1})	49.0 ± 5.8	2.20 ± 0.09
k_{-2} (s^{-1})	0.22 ± 0.04	0.0030 ± 0.0007
Effective K_i (μM)	1.9	1.6
Nimesulide		
Steady-state K_i (μM)	340 ± 70	410 ± 96
k_2 (s^{-1})	–	5.6 ± 0.1
k_{-2} (s^{-1})	–	0.0130 ± 0.0005
Effective K_i (μM)	–	0.95

$$E + I \underset{k_{-1}}{\overset{k_1}{\rightleftharpoons}} [EI] \underset{k_{-2}}{\overset{k_2}{\rightleftharpoons}} [EI^*] \xrightarrow{k_{inact}} EX$$

Scheme 3 Three-step irreverible mechanism

obtained from fitting the observed data to eqn (1) (see the Materials and methods section), and was found to be dependent on the concentration of inhibitor present in the preincubation mixture (inset to Figure 3b). The dependence of the observed rate on inhibitor concentration was fitted to eqn (2) in order to provide estimates for K_I and k_{inact} of 35 μM and 3.8 s^{-1} respectively (Table 1). Note that the equilibrium constant obtained from time-dependent inhibition is similar to that obtained from steady-state inhibition ($K_i = 20$ μM). This relationship suggests that steps involved in the formation of the initial rapid-equilibrium binary complex (i.e. in the absence of any pre-incubation) are similar to those steps that contribute to the concentration dependence observed during time-dependent inhibition (step 1 of Scheme 1).

Although the time-dependent inhibition of COX-2 by valdecoxib is consistent with an irreversible process, inactivation by diarylheterocyclic inhibitors is not accompanied by covalent modification of the enzyme. Several lines of evidence have demonstrated the reversible nature of this time-dependent process [15,23,25]. However, the dissociation rates are such that the release of inhibitor from the final tightly bound complex does not contribute to the kinetic data obtained from the present set of experiments. Therefore such time-dependent behaviour will be referred to as irreversible in the context of the present investigation. This will be addressed further in the Discussion section.

A k_{inact} value of 3.8 s^{-1} for time-dependent inhibition of COX-2 by valdecoxib is one of the fastest observed to date with COX-2-selective compounds. At concentrations $\geqslant 3$ μM the inhibition of COX-2 by valdecoxib is nearly complete following a 10 s preincubation with enzyme in the absence of substrate (Figure 3b). Note that the concentrations of inhibitor utilized for the analysis of steady-state inhibition (Figure 2b) are between ten and one hundred times higher than those utilized for the analysis of time-dependent inhibition. Thus it is likely that k_{inact} contributes to the inhibitory effect observed during steady-state experiments at higher inhibitor concentrations.

The steady-state and time-dependent inhibitory behaviour of celecoxib was also examined, and the respective kinetic constants are summarized in Table 1. Analysis of the steady-state inhibition of COX isoforms by celecoxib provided K_i values of 4.2 and 14 μM for COX-1 and COX-2 respectively, when a model for competitive inhibition was used. However, the data obtained from steady-state inhibition of COX-1 by celecoxib were better fitted to a model for non-competitive inhibition (results not shown). This is interpreted as the result of slow competitive binding, similar to that observed with valdecoxib.

Celecoxib demonstrates inhibitory behaviour that is distinct from valdecoxib in that the K_i value obtained from steady-state inhibition of COX-2 by celecoxib (14 μM) is five times larger than the K_I obtained from time-dependent inhibition (3.0 μM). This difference suggests that there is an additional step subsequent to the formation of the initial binary complex (Scheme 3), which

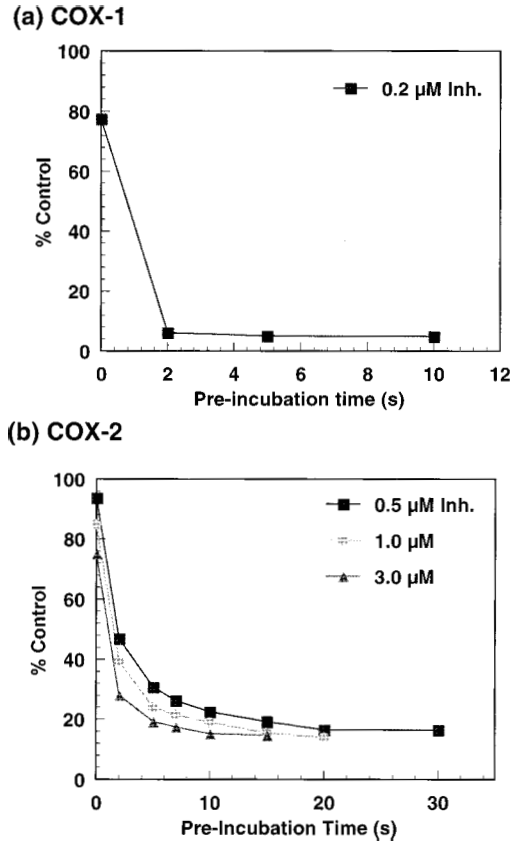

Figure 4 Time-dependent inhibition of (a) COX-1 and (b) COX-2 by SC-560

Assays were performed as described for Figure 3. The lines are drawn through the data points and do not correspond to monoexponential decays. Inh., inhibitor.

contributes to the concentration dependence observed during time-dependent inhibition [18]. It is estimated that the second equilibrium process contributes approximately 5-fold to the binding affinity afforded by the formation of the initial binary complex alone. This second step is then followed by a kinetically irreversible process, represented by k_{inact}, which becomes rate limiting at high concentrations of inhibitor.

In addition to examples of COX-2-selective inhibitors, the evaluation of structure–activity relationships within the diarylheterocyclic class also provided inhibitors that are more selective for COX-1 [11,14]. SC-560 (Figure 1) is an example of a diarylpyrazole containing a methyl ether in place of the sulphonamide group present in valdecoxib and celecoxib. The data obtained with COX-1 in the absence of any preincubation fitted reasonably well to a model for competitive inhibition (results not shown), despite a slight effect on V_{max}. The data obtained with COX-2 displayed a greater effect on V_{max}, which could be better accommodated by a model for non-competitive inhibition. However, the values predicted for K_m^{arach} and V_{max} by a non-competitive model were overestimated. As before, a V_{max} effect is interpreted as the result of slow competitive interactions. Analysis of the data using a model for competitive inhibition resulted in apparent K_i values of 0.1 μM with COX-1 and 1.8 μM with COX-2 (Table 1). SC-560 appears to be approximately 20-fold more potent against COX-1, based upon the comparison of steady-state K_i values. Note that the K_i value of 0.1 μM is approaching the concentration of enzyme in the assay. Therefore this value should be regarded as an approximation.

Unlike the COX-2-selective diarylheterocycles, SC-560 demonstrated time-dependent inhibition of both COX isoforms (Figure 4). Time-dependent inhibition of COX-1 by SC-560 was quite rapid, even at relatively low concentrations of inhibitor. As illustrated in Figure 4(a), enzyme activity was reduced from 70% of control in the absence of a preincubation to less than 10% following a 2 s preincubation with enzyme at an inhibitor concentration of 0.2 μM. Consequently, it was not possible to determine kinetic constants for the time-dependent inhibition of COX-1 by SC-560 using the present assay method. Furthermore, it is likely that this time-dependent process contributes to the apparent K_i obtained from the analysis of steady-state inhibition of COX-1 by SC-560.

Time-dependent inhibition of COX-2 by SC-560 was not as rapid as that observed with COX-1, permitting the collection of data over a period of approx. 30 s (Figure 4b). The loss of COX-2 activity following preincubation with SC-560 did not proceed to complete inhibition. Residual activity was observed even after prolonged incubation at relatively high concentrations of inhibitor. This kinetic behaviour is consistent with the presence of a slow reversible process subsequent to the formation of the initial rapid-equilibrium binary complex [30,32,33], as illustrated by Scheme 2. The loss of activity was reasonably well described by a monoexponential decay to a non-zero offset [eqn (3)]. The rate of decay was observed to increase with increasing inhibitor concentration but did not exhibit the expected concentration dependence. Additionally, the residual activity did not progressively approach zero as the concentration of inhibitor was increased. Such a change would have been expected as the final equilibrium position is forced further toward completion. As a result of these deviations, a satisfactory fit of the data to eqn (5) could not be obtained.

Examination of the reaction progress curves obtained with COX-1 and COX-2 in the presence of SC-560 demonstrated a dramatic increase in the time required to achieve maximal rate following the addition of substrate (results not shown). Typically, maximal rates of O_2 consumption were achieved within approximately 3 s following the addition of substrate. However, in the presence of 0.5 μM inhibitor the maximal rate of O_2 consumption catalysed by COX-2 was not achieved until 15–18 s after substrate addition. Similar delays in the time required to achieve maximal rate were also observed with COX-1. It is likely that the delay in reaching maximal rate is a consequence of the perturbation of an initial equilibrium that was established in the absence of substrate. Thus the time-dependent inhibition of COX enzymes by SC-560 is the result of a slow reversible process that favours COX-1.

The steady-state and time-dependent inhibitory behaviour of two typical NSAIDs were evaluated in order to provide a basis for comparison with results obtained with the diarylheterocyclic inhibitors. Meloxicam is a member of the enolic-acid family of NSAIDs (Figure 1). Results obtained during the steady-state inhibition of COX-1 by meloxicam were better described by a model for competitive inhibition, providing a K_i of 430 μM (Table 1). Despite the better fit to a competitive model, there was evidence for an inhibitory effect on V_{max}, as well as a slight degree of sigmoidal behaviour in direct plots of rate versus substrate at higher inhibitor concentrations (results not shown). Meloxicam was an even weaker inhibitor of COX-2, with a competitive K_i of 1150 μM (Table 1). In the case of COX-2 the extent of inhibition was such that it was not possible to distinguish any deviations from expected behaviour over the range of inhibitor concentrations examined.

Unlike the examples of COX-2-selective diarylheterocycles, meloxicam demonstrated time-dependent inhibition of both COX-1 and COX-2. In each case, the loss of enzymic activity

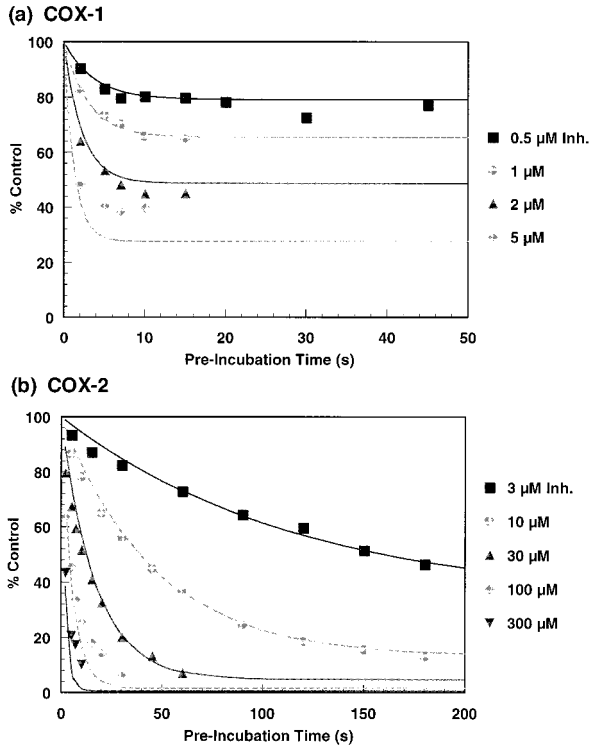

Figure 5 Time-dependent inhibition of (a) COX-1 and (b) COX-2 by meloxicam

Assays were performed as described for Figure 3. The curves drawn were obtained by global fitting of all data points to a single equation corresponding to a monoexponential decay with a non-zero offset, as defined by eqn (5). Note the deviation between observed and predicted behaviour at the highest concentrations of inhibitor (Inh.).

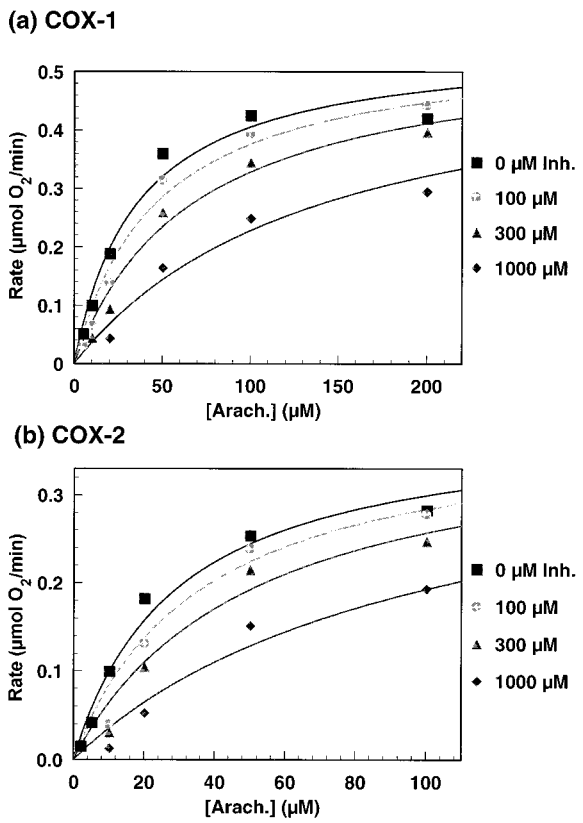

Figure 6 Direct plots of the maximal rate of O_2 consumption/min as a function of substrate concentration obtained at various concentrations of nimesulide with either (a) COX-1 or (b) COX-2

Assays and data analysis were performed as described for Figure 2. Arach., arachidonate; Inh., inhibitor.

following preincubation describes a monoexponential decay that does not proceed to completion (Figure 5). As discussed previously, this behaviour is consistent with the presence of a slow reversible process subsequent to the formation of the initial rapid-equilibrium binary complex (Scheme 2). In the case of COX-1, the observed rate of decay became too fast to measure at inhibitor concentrations above 5 μM. The rate of decay predicted from global fitting of the data to eqn (5) demonstrated a dependence on inhibitor concentration and the residual activity progressively approached complete inhibition as the inhibitor concentration was increased. Estimates of 49 and 0.22 s^{-1} for k_2 and k_{-2} respectively, were obtained for the slow reversible inhibition of COX-1. Based upon these values, the contribution of the second equilibrium provides a 220-fold increase in potency, relative to the formation of the rapid-equilibrium binary complex (effective $K_i = 1.9$ μM; cf. Table 1). In the case of COX-2, the rate of decay was much slower. Estimates of 2.2 and 0.003 s^{-1} for k_2 and k_{-2} respectively, were obtained by global fitting. These results suggest that the contribution of the second equilibrium results in an increase in potency for COX-2 of over 700-fold (effective $K_i = 1.6$ μM). Despite the large contributions to binding affinity provided by the second reversible step, note that the overall potencies for COX-1 and COX-2 are similar, as reflected by the effective K_i values. Thus although a slow reversible process contributes to the potency of meloxicam, this process does not provide selectivity for COX-1 or COX-2.

The time-dependent behaviour observed with meloxicam demonstrated deviations between observed and predicted behaviour at the highest concentrations of inhibitor examined (Figure 5). This is particularly evident from the data obtained with COX-1 where the residual activity does not decrease below 40% of control in the presence of 5 μM inhibitor. As was observed with SC-560, an increase in the time delay between the addition of substrate and the attainment of maximal rate was observed in the reaction progress curves obtained at the highest concentration of meloxicam (results not shown). Therefore the deviation between observed and predicted behaviour is interpreted as a consequence of the pertubation of an initial equilibrium established between enzyme and inhibitor by the addition of substrate.

Nimesulide (Figure 1) is another NSAID that has been reported to be a COX-2-selective inhibitor [34,35]. Analysis of the steady-state inhibitory behaviour demonstrated that nimesulide is a relatively weak inhibitor of both isoforms (Table 1). In the case of COX-1, the kinetic data obtained were reasonably well behaved at inhibitor concentrations as high as 300 μM and were consistent with a kinetic model for competitive inhibition ($K_i =$ 340 μM; Figure 6a). The observed data began to deviate from the expected rectangular hyperbola only after the inhibitor concentration was increased to 1 mM. Nimesulide did not demonstrate time-dependent inhibition of COX-1 (Figure 7a).

In the case of COX-2, the steady-state kinetic data obtained with nimesulide displayed distinct deviations from classical steady-state kinetic behaviour at inhibitor concentrations as low as 100 μM (Figure 6b). As observed previously, the data describe

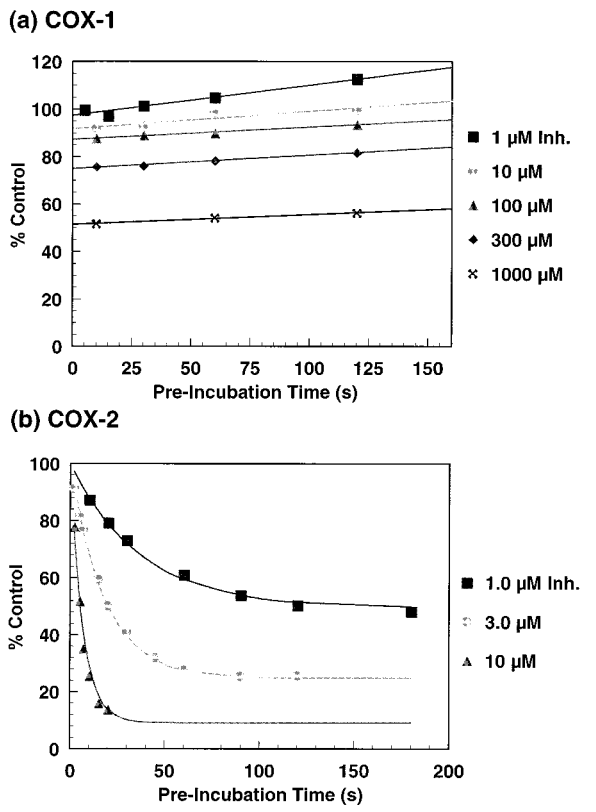

Figure 7 Time-dependent inhibition of (a) COX-1 and (b) COX-2 by nimesulide

Assays were performed as described for Figure 3. The curves drawn were obtained by global fitting of all data points to a single equation corresponding to a monoexponential decay with a non-zero offset, as defined by eqn (5). Inh., inhibitor.

a series of sigmoidal curves that suggest increasing contributions from a time-dependent inhibitory process at lower substrate concentrations. Fitting to a model for competitive inhibition provided a K_i estimate of 410 μM.

Nimesulide was demonstrated to be a potent time-dependent inhibitor of COX-2 (Figure 7b), as suggested by the non-classical steady-state kinetic behaviour. Time-dependent inhibition of COX-2 was observed at concentrations of nimesulide that were much lower than those utilized for the analysis of steady-state inhibition. The loss of enzymic activity following preincubation with nimesulide describes a monoexponential decay, which does not proceed to completion. The rate of decay demonstrated a dependence on inhibitor concentration, and the residual activity progressively approached complete inhibition as the inhibitor concentration was increased, indicating the presence of a slow reversible process subsequent to the formation of the initial binary complex (Scheme 2). Estimates for k_2 and k_{-2} of 5.6 and 0.013 s^{-1} respectively, were obtained by global fitting of all data to eqn (5). This slow equilibrium contributes to an increase in potency of approximately 430-fold (effective $K_i = 0.95$ μM) and is responsible for the selectivity demonstrated by nimesulide for COX-2. This is in contrast with SC-560, where a slow reversible process has been exploited to provide selectivity for COX-1.

DISCUSSION

Rome and Lands [17] were among the first to recognize the importance of time-dependent inhibition to potency against COX. Kinetic models for the analysis of time-dependent inhibition are typically comprised of a rapid reversible second-order reaction followed by a slow irreversible first-order reaction (Scheme 1). Such a two-step model is consistent with the steady-state and time-dependent inhibitory behaviour observed with valdecoxib on COX-2. Comparison of the respective kinetic constants demonstrates that the concentration dependence observed during both steady-state and time-dependent experiments is the result of a single rapid equilibrium between free enzyme and inhibitor. In addition, the equilibrium constant for reversible inhibition of COX-1 is similar to that for reversible inhibition of COX-2, suggesting that similar molecular interactions contribute to the rapid equilibrium binding of valdecoxib to both COX isoforms. Selectivity for COX-2 is provided by a slow irreversible step that does not contribute to the potency with COX-1.

In the case of celecoxib, the equilibrium constant for time-dependent inhibition is approximately 5-fold lower than that obtained during steady-state inhibition. This suggests that an additional equilibrium step contributes to the concentration dependence observed during preincubations of inhibitor with COX-2 (Scheme 3). These two steps appear to be kinetically indistinguishable during the inhibition of COX-2 with valdecoxib. As with valdecoxib, celecoxib's selectivity for COX-2 is provided by a slow irreversible step that does not contribute to the inhibition of COX-1 (k_{inact} of Scheme 3).

Results from X-ray crystallography have suggested that the selectivity for COX-2 demonstrated by diarylheterocycles, such as valdecoxib and celecoxib, is derived from an association of the phenylsulphonamide moiety within a side pocket present in the active site of COX-2 [36]. This side pocket is more accessible from the COX active site in COX-2 than in COX-1. Increased accessibility is, in part, the result of the substitution of a valine for an isoleucine found at position 523 in COX-1 [36]. The association of the phenylsulphonamide moiety within the side pocket of COX-2, but not COX-1, has been proposed to account for the selectivity of these molecules. Consistent with this interpretation, when the valine residue in COX-2 was mutated into an isoleucine residue, irreversible time-dependent inhibition of COX-2 by SC-58125, a close structural analogue of celecoxib, was abolished [24,33]. However, a slow reversible inhibitory process was still evident. This observation provides further support for the presence of two reversible steps preceding irreversible association within the active site (Scheme 3). The presence of multiple reversible steps that contribute to overall potency has been proposed previously for a variety of NSAIDs [32,37,38]. However, the diarylheterocycles provide the first examples of inhibitors that display three kinetically distinct processes [18,25].

It is likely that such slow reversible processes also contribute to the inhibition of COX-1 by diarylheterocycles [25]. Although there was no evidence for time-dependent inhibition of COX-1 by celecoxib or valdecoxib, the steady-state kinetic data obtained during the inhibition of COX-1 by these inhibitors were better described by a kinetic model for non-competitive inhibition. This behaviour is manifested as a V_{max} effect observed in plots of reaction rate versus substrate concentration. Similar kinetic behaviour has also been observed with other NSAIDs [29]. Multi-step equilibria, such as that illustrated in Scheme 2, can give rise to non-competitive steady-state inhibitory behaviour [31]. Therefore it is probable that additional equilibrium steps contribute to the inhibition of COX-1 by valdecoxib and celecoxib. However, the slow irreversible interactions characteristic of COX-2 inhibition by these compounds do not contribute to potency against COX-1.

SC-560 lacks the phenylsulphonamide moiety common to the COX-2-selective inhibitors. Analysis of time-dependent inhibition by SC-560 clearly demonstrated a slow reversible step subsequent to formation of the initial rapid-equilibrium binary complex with both COX isoforms (Scheme 2). This second equilibrium has been exploited by SC-560 to provide for selectivity against COX-1 rather than COX-2. Clearly, there are unique interactions within the respective active sites, independent of those provided by the side pocket, that can be utilized to distinguish between the COX isoforms.

In addition to the diarylheterocycles, several other NSAIDs also exhibit evidence for a two-step equilibrium during inhibition of COX. Time-dependent inhibition by meloxicam demonstrates slow reversible inhibition of both COX isoforms. However, these slower interactions appear comparable with both isoforms and do not provide for selectivity against either COX-1 or COX-2.

Similar to celecoxib and valdecoxib, nimesulide demonstrated time-dependent inhibition of COX-2, but not COX-1. However, this time-dependent behaviour was reversible, unlike the irreversible inhibition observed with the sulphonamide-containing diarylheterocycles. This suggests that the molecular interactions formed by nimesulide with COX-2 are probably different from those formed by celecoxib-like molecules. Results from mutagenesis studies are in agreement with this hypothesis. For example, mutation of valine to isoleucine at position 523 of COX-2 has only a modest effect on the time-dependent inhibition of nimesulide [24]. In contrast, the same mutation causes a dramatic difference in the kinetic profile of SC-58125 [24,33]. This suggests that the environment around Val^{523} and the side pocket is less important for the binding of nimesulide than for celecoxib and its analogues.

Observations from kinetics and structure can be combined together to arrive at a working model for COX inhibition [25]. According to this model, the overall inhibition of COX-2 by diarylheterocycles occurs in three distinct steps, as illustrated in Scheme 3. The first two steps represent reversible equilibrium processes, followed by an irreversible reaction that leads to the formation of a tightly bound enzyme–inhibitor complex (EX). The first reversible step probably represents the interaction of the inhibitor at the surface near the membrane-binding region of the enzyme, approximately 25 Å away from the active-site Tyr^{385} (1 Å ≡ 0.1 nm). This has been referred to as the lobby region, which acts as the entrance to a hydrophobic channel leading to the COX active site [39]. The lobby region is separated from the interior of the active site by a constriction formed by Tyr^{355} and Arg^{120}. While there is no direct structural evidence for initial binding of inhibitors at this lobby region, such interactions are likely to precede the formation of the optimized complex.

The second step of the inhibitor interaction with COX-2 in Scheme 3 could represent translocation of the inhibitor from the lobby to the COX active site. Additional protein conformational changes may also occur as part of this process. Crystal structures of NSAIDs bound to COX-1 and COX-2 demonstrate that protein conformational changes must occur during or after the binding of the inhibitor in the COX active site [36,40]. Typical non-selective NSAIDs, such as indomethacin, bind within the active site with the carboxylate of the inhibitor forming an ion-pair with the guanidinium group of Arg^{120}. Only a very small portion of the inhibitor is exposed to the solvent in the complex with COX-1 [40]. Thus it appears that the protein has wrapped around the inhibitor near the membrane-binding region.

For the COX-2-selective diarylheterocycles, the third and final step is likely to be a re-arrangement or fine-tuning of the inhibitor in the active site, which ultimately results in strong interactions of the phenylsulphonamide or phenylsulphone group with protein residues in the side pocket. We propose that these changes occur during the third irreversible kinetic step of inhibitor binding. The crystallographic structure of SC-558 bound to COX-2 [36] most likely represents the structure of this final complex (EX of Scheme 3).

Several lines of evidence support this working model. As described earlier, mutation of residues in the side pocket of COX-2 has a profound effect on the irreversible time-dependent inhibition of phenylsulphonamide-containing diarylheterocycles. The second line of support comes from observations with those inhibitors that do not have a phenylsulphonamide or phenylsulphone group, such as SC-560. According to the above model, these inhibitors should not be able to undergo the third irreversible step illustrated in Scheme 3. Consistent with this interpretation, some residual activity is always present after prolonged preincubation of SC-560 with both COX-1 and COX-2. Additionally, the time required to reach maximal velocity following the addition of substrate is increased when in the presence of inhibitor. Both of these observations support the contention that this time-dependent process is reversible (Scheme 2).

This working model also appears to account for the kinetic behaviour of acidic NSAIDs, such as flurbiprofen and indomethacin [32,37,38]. The structures of flurbiprofen and indomethacin complexes show that they have very few interactions in the side pocket of COX-2 [36]. Obviously, the structural basis for the time-dependence observed with these two inhibitors must be completely different from that of COX-2-selective diarylheterocyclic inhibitors. One common theme in the structures of these acidic NSAIDs is the ion-pairing interaction formed between the carboxylate of the inhibitor and Arg^{120} of the enzyme. This interaction probably represents the structural basis for the time-dependent inhibition observed with these acidic NSAIDs, as described by Rome and Lands [17]. Consistent with this interpretation, flurbiprofen has been demonstrated to be a reversible inhibitor of the $Arg^{120} \rightarrow Gln$ mutant [41]. Elimination of the ion-pairing ability by site-directed mutagenesis abolished the time-dependent inhibition typically observed with these NSAIDs.

Irreversible time-dependent inhibition of COX-2 by selective diarylheterocycles implies that the reaction proceeds to complete inactivation. While the kinetic data presented are consistent with an irreversible process, it is well recognized that inactivation is not the result of covalent modification of the enzyme, as is the case with aspirin inactivation of COX [42]. It has been demonstrated that, upon denaturation of the inactivated complex, the inhibitor is released unaltered ([15,23], and J. K. Gierse, unpublished work). Recent results from fluorescence quenching experiments [25], and the binding of radiolabelled celecoxib to COX-2 (W. F. Hood, J. K. Gierse, P. C. Isakson, J. R. Kiefer, R. G. Kurumbail, K. Seibert and J. B. Monahan, unpublished work) have further demonstrated the reversible nature of inhibition by these COX-2-selective diarylheterocycles. The observed half-times for inhibitor release from the final tightly bound complex are in vast excess of the time scale used in the current kinetic experiments. Therefore the kinetics for time-dependent inhibition of COX-2 by selective diarylheterocycles closely approximate those expected for an irreversible process under the current experimental conditions.

In several cases, a sigmoidal dependence of rate versus arachidonate concentration was observed at the highest concentrations of inhibitor utilized during the examination of steady-state inhibition. Similar kinetic behaviour has been reported previously for COX-1 [43,44]; however, these results were obtained in the absence of inhibitors. The observed behaviour

was interpreted as the result of feedback regulation via the coupling of COX and the peroxidase reactions [44]. In the present case, sigmoidal behaviour was observed under conditions where the inhibitor concentrations utilized during the examination of steady-state inhibition were much higher than those utilized during the examination of time-dependent inhibition. In such circumstances, the observed rate constant for time-dependent inhibition would approach or exceed the response time of the oxygraph instrument. Thus it is likely that the extent of inhibition observed in steady-state experiments will include contributions from time-dependent processes. This contribution is expected to be inversely proportional to the concentration of substrate and could account for the observed sigmoidal dependence of rate on substrate concentration.

Kinetic constants for the steady-state inhibition of COX-1 and COX-2 by celecoxib have been reported previously [18]. The K_i values reported were calculated graphically from double-reciprocal plots of reaction velocity versus substrate concentration. The graphical method for the determination of inhibition constants places greater statistical weighting on observations obtained at the lowest substrate concentrations. In the present study, kinetic constants were calculated by non-linear least-squares fitting to a multi-parameter mathematical model for competitive inhibition, with equal weighting applied to all data. Differences between previously reported kinetic constants and those reported in the present paper are the result of differences in statistical weighting used by the respective numerical methods, and reflect deviations between observed data and fitted results at the lowest substrate concentrations, as discussed above.

In conclusion, comparison of kinetic data obtained during steady-state and time-dependent inhibition of COX-1 and -2 by a series of diarylheterocycles has provided evidence for a three-step reversible kinetic model for COX inhibition. The first step is interpreted as the second-order binding of inhibitor to enzyme near the solvent-accessible opening of the hydrophobic channel [36,39], commonly referred to as the lobby region [5,25]. The second kinetic process is interpreted as corresponding to the translocation of inhibitor along the length of this channel and subsequent association within the COX active site. Both of these processes are probably common to COX-1 and COX-2 during inhibition by the vast majority of NSAIDs. Depending on the magnitude of the relative rate constants the individual steps may not appear distinct, as was observed with valdecoxib. A third kinetic process, which appears to be irreversible, is only observed during the inhibition of COX-2 by diarylheterocycles that contain a phenylsulphonamide or a phenylsulphone moiety. This process is interpreted as the formation of the tightly bound enzyme–inhibitor complex, which involves the optimization of inhibitor and protein conformational changes in the active site and the side pocket. This kinetic model can satisfactorily account for the different types of inhibitory behaviour observed with most NSAIDs against both COX-1 and COX-2 when appropriate estimates for each of the microscopic rate constants are provided.

We would like to acknowledge Dr Larry Marnett for helpful discussions regarding the structure and mechanism of COX enzymes, and Dr Arthur Wittwer for the modelling of time-dependent inhibition. We also thank Jennifer Pierce and Rodney Combs for providing Sf9 insect cell cultures expressing murine COX-2.

REFERENCES

1 Vane, J. R. (1974) Mode of action of aspirin and similar compounds. In Prostaglandin Synthase Inhibitors (Robinson, J. H. and Vane, J. R., eds.), pp. 155–163, Raven Press, New York
2 Smith, W. L. and Marnett, L. J. (1991) Prostaglandin endoperoxide synthase: structure and catalysis. Biochim. Biophys. Acta **1083**, 1–17
3 Smith, W. L., Garavito, R. M. and DeWitt, D. L. (1996) Prostaglandin endoperoxide H synthases (cyclooxygenases)-1 and -2. J. Biol. Chem. **271**, 33157–33160
4 DuBois, R. N., Abramson, S. B., Crofford, L., Gupta, R. A., Simon, L. S., van de Putte, L. B. A. and Lipsky, P. E. (1998) Cyclooxygenase in biology and disease. FASEB J. **12**, 1063–1073
5 Marnett, L. J., Rowlinson, S. W., Goodwin, D. C., Kalgutkar, A. S. and Lanzo, C. A. (1999) Arachidonic acid oxygenation by COX-1 and COX-2: Mechanisms of catalysis and inhibition. J. Biol. Chem. **274**, 22903–22906
6 Seibert, K. and Masferrer, J. L. (1994) Role of inducible cyclooxygenase (COX-2) in inflammation. Receptor **4**, 17–23
7 Vane, J. R., Bakhe, Y. S. and Botting, R. M. (1998) Cyclooxygenases 1 and 2. Annu. Rev. Pharmacol. Toxicol. **38**, 97–120
8 Lecomte, M., Laneuville, O., Ji, C., DeWitt, D. L. and Smith, W. L. (1994) Acetylation of human prostaglandin endoperoxide synthase-2 (cyclooxygenase-2) by aspirin. J. Biol. Chem. **269**, 13207–13215
9 Warner, T. D., Giuliano, F., Vojnovic, I., Bukasa, A., Mitchell, J. A. and Vane, J. R. (1999) Nonsteroid drug selectivities for cyclo-oxygenase-1 rather than cyclo-oxygenase-2 are associated with human gastrointestinal toxicity: A full *in vitro* analysis. Proc. Natl. Acad. Sci. U.S.A. **96**, 7563–7568
10 Gierse, J. K., Hauser, S. D., Creely, D. P., Koboldt, C., Rangwala, S. H., Isakson, P. C. and Seibert, K. (1995) Expression and selective inhibition of the constitutive and inducible forms of human cyclo-oxygenase. Biochem. J. **305**, 479–484
11 Smith, C. J., Zhang, Y., Koboldt, C. M., Muhammad, J., Zweifel, B. S., Shaffer, A., Talley, J. J., Masferrer, J. L., Seibert, K. and Isakson, P. C. (1998) Pharmacological analysis of cyclooxygenase-1 in inflammation. Proc. Natl. Acad. Sci. U.S.A. **95**, 13313–13318
12 Gans, K. R., Galbraith, W., Roman, R. J., Haber, S. B., Kerr, J. S., Schmidt, W. K., Smith, C., Hewes, W. E. and Ackerman, N. R. (1990) Anti-inflammatory and safety profile of DuP 697, a novel orally effective prostaglandin synthesis inhibitor. J. Pharmacol. Exp. Ther. **254**, 180–187
13 Futaki, N., Takahashi, S., Yokoyama, M., Aria, I., Higuchi, S. and Otomo, S. (1994) NS-398, a new anti-inflammatory agent, selectively inhibits prostaglandin G/H synthase/cyclooxygenase (COX-2) activity *in vitro*. Prostaglandins **47**, 55–59
14 Penning, T. D., Talley, J. J., Bertenshaw, S. R., Carter, J. S., Collins, P. W., Doctor, S., Graneto, M. J., Lee, L. F., Malecha, J. W., Miyashiro, J. M. et al. (1997) Synthesis and biological evaluation of the 1,5-diarylpyrazole class of cyclooxygenase-2 inhibitors: identification of 4-[5-(4-methylphenyl)-3-(trifluoromethyl)-1H-pyrazol-1-yl]benzenesulfonamide (SC-58635, celecoxib). J. Med. Chem. **40**, 1347–1365
15 Reindeau, D., Percival, M. D., Boyce, S., Brideau, C., Charleson, S., Cromlish, W., Ethier, D., Evans, J., Falgueyret, J.-P., Ford-Hutchinson, A. W. et al. (1997) Biochemical and pharmacological profile of a tetrasubstituted furanone as a highly selective COX-2 inhibitor. Br. J. Pharmacol. **121**, 105–117
16 Chan, C.-C., Boyce, S., Brideau, C., Charleson, S., Cromlish, W., Ethier, D., Evans, J., Ford-Hutchinson, A. W., Forrest, M. J., Gauthier, J. Y. et al. (1999) Rofecoxib [Vioxx, MK-0966; 4-(4′-methylsulfonylphenyl)-3-phenyl-2-(5H)-furanone]: a potent and orally active cyclooxygenase-2 inhibitor. Pharmacological and biochemical profiles. J. Pharmacol. Exp. Ther. **290**, 551–560
17 Rome, L. H. and Lands, W. E. M. (1975) Structural requirements for time-dependent inhibition of prostaglandin biosynthesis by anti-inflammatory drugs. Proc. Natl. Acad. Sci. U.S.A. **72**, 4863–4865
18 Gierse, J. K., Koboldt, C. M., Walker, M. C., Seibert, K. and Isakson, P. C. (1999) Kinetic basis for selective inhibition of cyclo-oxygenases. Biochem. J. **339**, 607–614
19 Van Der Ouderaa, F. J., Buytenhek, M., Nugteren, D. H. and Van Dorp, D. A. (1980) Acetylation of prostaglandin endoperoxide synthetase with acetylsalicylic acid. Eur. J. Biochem. **109**, 1–8
20 Kalgutkar, A. S., Crews, B. C., Rowlinson, S. W., Garner, C., Seibert, K. and Marnett, L. J. (1998) Aspirin-like molecules that covalently inactivate cyclooxygenase-2. Science (Washington, D.C.) **280**, 1268–1270
21 Cryer, B. and Dubois, A. (1998) The advent of highly selective inhibitors of cyclooxygenase – a review. Prostaglandins Other Lipid Mediators **56**, 341–361
22 Battistini, B., Botting, R. and Bakhle, Y. S. (1994) COX-1 and COX-2: Toward the development of more selective NSAIDs. Drug News & Perspect. **7**, 501–511
23 Copeland, R. A., Williams, J. M., Giannaras, J., Nurnberg, S., Covington, M, Pinto, D., Pick, S. and Trzaskos, J. M. (1994) Mechanism of selective inhibition of the inducible isoform of prostaglandin G/H synthase. Proc. Natl. Acad. Sci. U.S.A. **91**, 11202–11206
24 Gierse, J. K., McDonald, J. J., Hauser, S. D., Rangwala, S. H., Koboldt, C. M. and Seibert, K. (1996) A single amino acid difference between cyclooxygenase-1 (COX-1) and -2 (COX-2) reverses the selectivity of COX-2 specific inhibitors. J. Biol. Chem. **271**, 15810–15814
25 Lanzo, C. A., Sutin, J., Rowlinson, S., Talley, J. and Marnett, L. J. (2000) Fluorescence quenching analysis of the association and dissociation of a diarylheterocycle to cyclooxygenase-1 and cyclooxygenase-2: Dynamic basis of cyclooxygenase-2 selectivity. Biochemistry **39**, 6228–6234

26 Talley, J. J. (1999) Isoxazole Compounds as Cyclooxygenase Inhibitors. U.S. Patent #5,859,257
27 Leatherbarrow, R. J. (1992) GraFit v 4.0, Erithacus Software Ltd, Staines, U.K.
28 Kitz, R. and Wilson, I. B. (1962) Esters of methanesulfonic acid as irreversible inhibitors of acetylcholinesterase. J. Biol. Chem. **237**, 3245–3249
29 Ouellet, M. and Percival, M. D. (1995) Effect of inhibitor time-dependency on selectivity towards cyclooxygenase isoforms. Biochem. J. **306**, 247–251
30 Huang, Z.-F., Wun, T.-C. and Broze, G. J. (1993) Kinetics of factor Xa inhibition by tissue factor pathway inhibitor. J. Biol. Chem. **268**, 26950–26955
31 Morrison, J. F. and Walsh, C. T. (1988) The behavior and significance of slow-binding enzyme inhibitors. Adv. Enzymol. Rel. Areas Mol. Biol. **61**, 201–301
32 Callan, O. H., So, O.-Y. and Swinney, D. C. (1996) The kinetic factors that determine the affinity and selectivity for slow binding inhibition of human prostaglandin H synthase 1 and 2 by indomethacin and flurbiprofen. J. Biol. Chem. **271**, 3548–3554
33 Guo, Q., Wang, L.-H., Ruan, K.-H. and Kulmacz, R. J. (1996) Role of Val509 in time-dependent inhibition of human prostaglandin H synthase-2 cyclooxygenase activity by isoform-selective agents. J. Biol. Chem. **271**, 19134–19139
34 Bennett, A. (1999) Overview of nimesulide. Rheumatology **38** (supplement 1), 1–3
35 Shah, A. A., Murray, F. E. and Fitzgerald, D. J. (1999) Overview of nimesulide. Rheumatology **38** (supplement 1), 19–23
36 Kurumbail, R. G., Stevens, A. M., Gierse, J. K., McDonald, J. J., Stegeman, R. A., Pak, J. Y., Gildehaus, D., Miyashiro, J. M., Penning, T. D., Seibert, K. et al. (1996) Structural basis for selective inhibition of cyclooxygenase-2 by anti-inflammatory agents. Nature (London) **384**, 644–648

Received 18 January 2001/9 April 2001; accepted 16 May 2001

37 Wong, E., Bayly, C., Waterman, H. L., Riendeau, D. and Mancini, J. A. (1997) Conversion of prostaglandin G/H synthase-1 into an enzyme sensitive to PGHS-2-selective inhibitors by a double His513 → Arg and Ile523 → Val mutation. J. Biol. Chem. **272**, 9280–9286
38 So, O. Y., Scarafia, L. E., Mak, A. Y., Callan, O. H. and Swinney, D. C. (1998) The dynamics of prostaglandin H synthases. Studies with prostaglandin H synthase 2 Y355F unmask mechanisms of time-dependent inhibition and allosteric activation. J. Biol. Chem. **273**, 5801–5807
39 Picot, D., Loll, P. J. and Garavito, R. M. (1994) The X-ray crystal structure of the membrane protein prostaglandin H2 synthase-1. Nature (London) **367**, 243–249
40 Loll, P. J., Picot, D., Ekabo, O. and Garavito, R. M. (1996) Synthesis and use of iodinated nonsteroidal antiinflammatory drug analogs as crystallographic probes of the prostaglandin H2 synthase cyclooxygenase active site. Biochemistry **35**, 7330–7340
41 Bhattacharyya, D. K., Lecomte, M., Rieke, C. J., Garavito, R. M. and Smith, W. L. (1996) Involvement of arginine 120, glutamate 524, and tyrosine 355 in the binding of arachidonate and 2-phenylpropionic acid inhibitors to the cyclooxygenase active site of ovine prostaglandin endoperoxide H synthase-1. J. Biol. Chem. **271**, 2179–2184
42 Roth, G. J., Stanford, N. and Majerus, P. W. (1975) Acetylation of prostaglandin synthase by aspirin. Proc. Natl. Acad. Sci. U.S.A. **72**, 3073–3076
43 Swinney, D. C., Mak, A. Y., Barnett, J. and Ramesha, C. S. (1997) Differential allosteric regulation of prostaglandin H synthase 1 and 2 by arachidonic acid. J. Biol. Chem. **272**, 12393–12398
44 Chen, W., Pawelek, T. R. and Kulmacz, R. J. (1999) Hydroperoxide dependence and cooperative cyclooxygenase kinetics in prostaglandin H synthase-1 and -2. J. Biol. Chem. **274**, 20301–20306